Superconductivity in Multilayer Perovskite: Weak Coupling Analysis

Shigeru Koikegami * and Takashi Yanagisawa

Nanoelectronics Research Institute, AIST Tsukuba Central 2, Tsukuba 305-8568, Japan

(Received December 3, 2005)

We investigate the superconductivity of a three-dimensional d-p model with a multilayer perovskite structure on the basis of the second-order perturbation theory within the weak coupling framework. Our model has been designed with multilayer high-T_c superconducting cuprates in mind. In our model, multiple Fermi surfaces appear, and the component of a superconducting gap function develops on each band. We have found that the multilayer structure can stabilize the superconductivity in a wide doping range.

KEYWORDS: superconductivity, three-dimensional d-p model, multilayer perovskite, second-order perturbation theory

1. Introduction

In the last decade, high-T_c superconducting cuprates (HTSCs) with multilayer structure have been investigated extensively by various experimental methods.[1–3] Multilayer cuprates typically have higher T_c than single-layer ones. The nuclear magnetic resonance (NMR) measurement systematically reveals the local hole concentration on each layer of the multilayer HTSCs. In previous excellent studies,[4,5] each layer has been crystallographically classified into an outer or inner CuO_2 plane in a unit cell. The authors found the relationship between the difference in the local hole concentration among these two types of planes and T_c, and they considered the condition in which T_c can be maximized. The results suggest that multiple Fermi surfaces are involved in superconductivity, and that an extensive theory on multilayer materials should be constructed on the basis of the model with multibands.

The above NMR study mainly revealed the characteristic of the multilayer compounds for $n \geq 3$, where n is the number of CuO_2 planes per unit cell. The characteristic feature of multiband systems can also appear explicitly in a bilayer compound. In $Bi_2Sr_2CaCu_2O_{8+\delta}$ (Bi2212), which is another typical bilayer material, the high-resolution angle-resolved-photoemission spectroscopy (ARPES) successfully revealed the doubling of a band near the Fermi level.[6,7] This splitting is negligible along the $(0,0) \rightarrow (\pi,\pi)$ nodal line and maximum at $(\pi,0)$ in momentum space. This momentum dependence of energy splitting is qualitatively consistent with the LDA prediction for $YBa_2Cu_3O_7$,[8] which is another bilayer material. This LDA calculation predicted that a Cu $4s$ orbital has a transfer integral between that in the other layer. This interlayer coupling causes a single band to split into antibonding and bonding bands.

*E-mail address : shigeru.koikegami@aist.go.jp

A multilayer model has been theoretically studied since the early 1990s by fluctuation exchange (FLEX) approximation[9] and by quantum Monte Carlo (QMC) simulation[9,10] on the basis of the two-dimensional (2D) multilayer Hubbard model. These studies have shown that the $d_{x^2-y^2}$-wave pairing correlations are reduced by interlayer transfer, which is independent of the in-plane momenta, k_x and k_y. However, when we introduce interlayer transfer into our model, it is important to consider the symmetry of interlayer transfer integrals in which Cu 4*s* electrons participate. Liechtenstein *et al.* considered this point and studied the extended Hubbard model with anisotropic interlayer hopping, using the FLEX approximation.[11] Although they could not reproduce the experimental result of bilayer materials having higher T_c than single-layer ones, their work should be appreciated as the first theoretical analysis of the superconductivity of realistic multilayer systems. All the theoretical works have been done on the basis of the 2D model Hamiltonian. We feel that we should investigate the *three-dimensional* model Hamiltonian with anisotropic interlayer hopping to estimate T_c of multilayer materials.

In this study, we investigate the superconductivity of multilayer perovskite. We adopt the three-dimensional (3D) d-p model with anisotropic interlayer transfers as our model Hamiltonian. In our model, we introduce such a small on-site Coulomb interaction that the second-order perturbation theory (SOPT) can be justified. We can treat the superconductivity within the weak coupling analysis because, in our model, the effective interaction for Cooper pairing is so small that only the electrons on the Fermi surface are involved in the superconductivity. The weak coupling formalism for the repulsive interaction model, since the pioneering work by Kohn and Luttinger,[12] has been developed by many theorists .[13–17] Recently, this formalism was applied, by Kondo, to the 2D Hubbard model with the formulation applicable even for the case with a very small effective interaction.[18] We apply Kondo's formulation to our model with multiple Fermi surfaces, and clarify how the superconducting gap depends on n of layers. We can show that the calculation on the basis of 3D model Hamiltonian is requisite for the true estimation of T_c of multilayer materials. Our obtained results are not only to be compared with the actual T_c of multilayer materials but to be considered as a guide for designing materials with high T_c.

2. Formulation

We can decompose our 3D d-p model with the n-layer perovskite structure into several parts as follows:

$$H = \sum_{l=1}^{n} [\, H_l^0 + H_{l+1,\,l}^0 + H_l' - \mu \sum_{\boldsymbol{k}\sigma} (d_{\boldsymbol{k}\,l\sigma}^{\dagger} d_{\boldsymbol{k}\,l\sigma} + p_{\boldsymbol{k}\,l\sigma}^{x\dagger} p_{\boldsymbol{k}\,l\sigma}^{x} + p_{\boldsymbol{k}\,l\sigma}^{y\dagger} p_{\boldsymbol{k}\,l\sigma}^{y}) \,],$$

(1)

where $d_{\boldsymbol{k}l\sigma}$ ($d^{\dagger}_{\boldsymbol{k}l\sigma}$), $p^{x}_{\boldsymbol{k}l\sigma}$ ($p^{x\dagger}_{\boldsymbol{k}l\sigma}$) and $p^{y}_{\boldsymbol{k}l\sigma}$ ($p^{y\dagger}_{\boldsymbol{k}l\sigma}$) are the annihilation (creation) operators for d-, p^x- and p^y-electrons of momentum $\boldsymbol{k}$ and spin $\sigma = \{\uparrow, \downarrow\}$ on the l-th layer, respectively. We define $n+1 \equiv 1$, and the chemical potential is represented by μ. The noninteracting parts in eq. (1), i.e., H^0_l and $H^0_{l+1,l}$, are represented by

$$H^0_l = \sum_{\boldsymbol{k}\sigma} \left(d^{\dagger}_{\boldsymbol{k}l\sigma}\, p^{x\dagger}_{\boldsymbol{k}l\sigma}\, p^{y\dagger}_{\boldsymbol{k}l\sigma} \right) \begin{pmatrix} \Delta_l & \zeta^x_{\boldsymbol{k}} & \zeta^y_{\boldsymbol{k}} \\ -\zeta^x_{\boldsymbol{k}} & 0 & \zeta^p_{\boldsymbol{k}} \\ -\zeta^y_{\boldsymbol{k}} & \zeta^p_{\boldsymbol{k}} & 0 \end{pmatrix} \begin{pmatrix} d_{\boldsymbol{k}l\sigma} \\ p^x_{\boldsymbol{k}l\sigma} \\ p^y_{\boldsymbol{k}l\sigma} \end{pmatrix} \tag{2}$$

and

$$H^0_{l+1,l} = \begin{cases} \sum_{\boldsymbol{k}\sigma} \zeta^z_{\boldsymbol{k}}\, d^{\dagger}_{\boldsymbol{k}\,l+1\sigma} d_{\boldsymbol{k}l\sigma} + \text{h.c.} & l = n \\ \sum_{\boldsymbol{k}\sigma} \zeta^d_{\boldsymbol{k}}\, d^{\dagger}_{\boldsymbol{k}\,l+1\sigma} d_{\boldsymbol{k}l\sigma} + \text{h.c.} & l < n \end{cases} . \tag{3}$$

In eqs. (2) and (3) we take the lattice constant of the square lattice formed of Cu sites, a, as the unit length. Using it, we can represent $\zeta^p_{\boldsymbol{k}} = 4t_{pp} \sin\frac{k_x}{2} \sin\frac{k_y}{2}$, $\zeta^x_{\boldsymbol{k}} = 2\mathrm{i}t_{dp} \sin\frac{k_x}{2}$, $\zeta^y_{\boldsymbol{k}} = 2\mathrm{i}t_{dp} \sin\frac{k_y}{2}$, $\zeta^z_{\boldsymbol{k}} = t_{\perp} \cos\frac{k_x}{2} \cos\frac{k_y}{2} e^{\mathrm{i}k_z r_a}$, and $\zeta^d_{\boldsymbol{k}} = \frac{t_{dd}}{4}(\cos k_x - \cos k_y)^2 e^{\mathrm{i}k_z r_b}$, where $r_a = \frac{c_a}{c_a+(n-1)c_b}$ and $r_b = \frac{c_b}{c_a+(n-1)c_b}$. c_a and c_b represent the distances among CuO_2 planes, as shown in Fig. 1. Hereafter, we use 'IP' and 'OP' as abbreviations for inner CuO_2 planes ($1 < l < n$) and outer CuO_2 planes ($l = 1$ or n), respectively. Δ_l is the hybridization gap energy on the l-th layer between d- and p-orbitals. When $n \geq 3$, our model has several crystallographically inhomogeneous CuO_2 planes, and Δ_l varies according to l. We can define Δ_l as

$$\Delta_l = \begin{cases} \Delta_{dp} & l = 1 \text{ or } n \\ \Delta_{dp} - \frac{\alpha}{r_a} & 1 < l < n \end{cases} , \tag{4}$$

where α is the constant chosen so as to reproduce the difference in doped carriers between OP and IP. We consider only the on-site Coulomb repulsion among d-electrons. Thus, the interacting part H'_l in eq. (1) is described as

$$H'_l = \frac{U}{N} \sum_{\boldsymbol{k}\boldsymbol{k}'\boldsymbol{q}} d^{\dagger}_{\boldsymbol{k}+\boldsymbol{q}\,l\uparrow} d^{\dagger}_{\boldsymbol{k}'-\boldsymbol{q}\,l\downarrow} d_{\boldsymbol{k}'\,l\downarrow} d_{\boldsymbol{k}\,l\uparrow}. \tag{5}$$

In eq. (5), N is the number of $\boldsymbol{k}$-space lattice points in the first Brillouin zone (FBZ), which is equal to the number of Cu sites in the real space.

In the following part, we assume that only the electrons on the Fermi surface of the same band can have singlet pair instability. For our n-layer model, n d-like bands always intersect with the Fermi level. Thus, according to the BCS theory, we have the following self-consistent

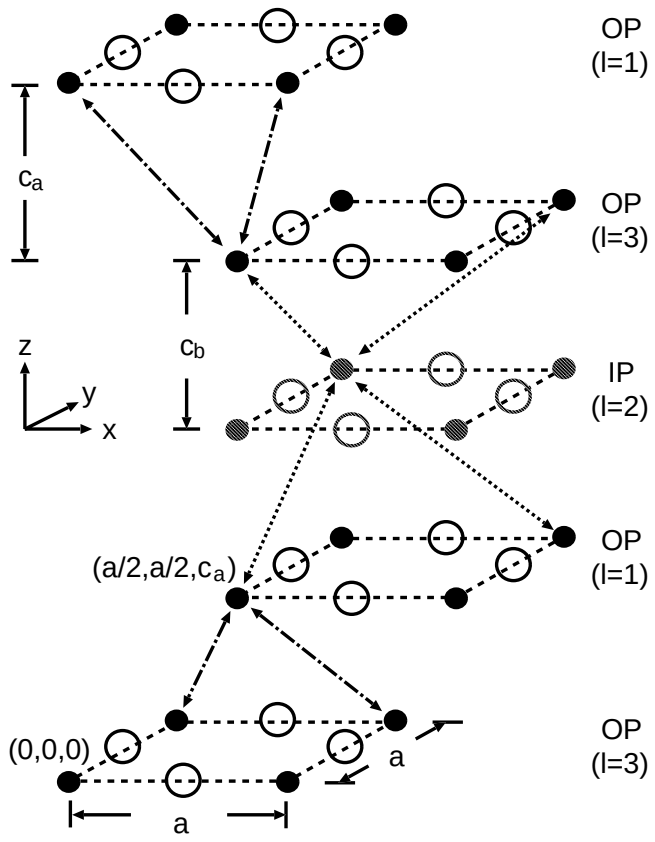

Fig. 1. Crystal structure modeled after trilayered perovskite. Filled (Open) circles represent copper (oxygen) cites. Dotted (Dot-dashed) arrows conecting copper cites correspond to $\zeta^d_{\boldsymbol{k}}$ ($\zeta^z_{\boldsymbol{k}}$) in the text.

equation for the pair function on the λ-th d-like band, $\Phi_{\boldsymbol{k}\lambda}$:

$$\Phi_{\boldsymbol{k}\lambda} = -\frac{1}{2N}\sum_{ij\boldsymbol{k}'\nu} V_{ij}(\boldsymbol{k}+\boldsymbol{k}')\frac{z_{i\lambda}(\boldsymbol{k})z_{j\nu}(\boldsymbol{k}')}{\sqrt{\left(\varepsilon_{\boldsymbol{k}'\nu}-\mu\right)^2+\left(\Phi_{\boldsymbol{k}'\nu}\right)^2}}\,\Phi_{\boldsymbol{k}'\nu}, \tag{6}$$

where $i,j=1,\ldots,n$ (layer indices) and $\lambda,\nu=1,\ldots,n$ (d-like band indices). $V_{ij}(\boldsymbol{q})$ represents the effective singlet pair scattering between a d-electron on the i-th layer and one on the j-th layer. $\varepsilon_{\boldsymbol{k}\nu}$ represents the energy dispersion of the ν-th d-like band, and $z_{i\lambda}(\boldsymbol{k})$ represents the matrix element of unitary transformation. They are obtained by solving the eigenequation for the noninteracting part in eq. (1). We set $\Phi_{\boldsymbol{k}\lambda} = \Delta_{\rm sc}\cdot\Psi_{\boldsymbol{k}\lambda}$, where $\Delta_{\rm sc}$ denotes the magnitude of $\Phi_{\boldsymbol{k}\lambda}$ and $\Psi_{\boldsymbol{k}\lambda}$ represents its $\boldsymbol{k}$-dependence on the λ-th d-like band. On the basis of Kondo's argument,[18] retaining only the divergent term, we can rewrite eq. (6) as

$$\begin{aligned}&\Psi_{\boldsymbol{k}\lambda} = \\ &\log_e \Delta_{\rm sc}\cdot\frac{1}{N}\sum_{ij\boldsymbol{k}'\nu} V_{ij}(\boldsymbol{k}+\boldsymbol{k}')z_{i\lambda}(\boldsymbol{k})z_{j\nu}(\boldsymbol{k}')\delta(\varepsilon_{\boldsymbol{k}'\nu}-\mu)\Psi_{\boldsymbol{k}'\nu}\end{aligned} \tag{7}$$

for very small $\Delta_{\rm sc}$. Equation (7) is a homogeneous integral equation for $\Psi_{\boldsymbol{k}\lambda}$ with the eigenvalue of $1/\log\Delta_{\rm sc}$. We are interested in obtaining the most stable superconducting state, thus we

must find the eigenvector $\Psi_{\boldsymbol{k}\lambda}$ with the smallest eigenvalue $1/\log\Delta_{\rm sc}$ using eq. (7) when $\Delta_{\rm sc}$ is maximum. In our previous paper, we confirmed that the most stable pairing state near half-filling is the $d_{x^2-y^2}$-wave, by a similar approach based on 2D d-p model.[19] Hence, when we assume that

$$\Psi_{\boldsymbol{k}\lambda} = a_\lambda(k_z)(\cos k_x - \cos k_y), \tag{8}$$

we can safely reduce our original eigenvalue problem for $\Psi_{\boldsymbol{k}\lambda}$ to an eigenvalue problem for $a_\lambda(k_z)$ in order to seek only the most stable pairing state. Furthermore, considering the symmetry of $\Psi_{\boldsymbol{k}\lambda}$ in eq. (8), we can take

$$\begin{aligned} V_{ij}(\boldsymbol{q}) &= U^2\chi_{ij}(\boldsymbol{q}) \\ &= \frac{U^2}{N}\sum_{\boldsymbol{k}\xi\eta} z_{i\xi}(\boldsymbol{q}+\boldsymbol{k}) z_{j\eta}(\boldsymbol{k}) \frac{(1-f_{\boldsymbol{q}+\boldsymbol{k}\xi})\, f_{\boldsymbol{k}\eta}}{\varepsilon_{\boldsymbol{q}+\boldsymbol{k}\xi} - \varepsilon_{\boldsymbol{k}\eta}} \end{aligned} \tag{9}$$

within SOPT. In eq. (9),

$$f_{\boldsymbol{k}\eta} = \frac{1}{2}\left[1 - \tanh\left(\frac{\varepsilon_{\boldsymbol{k}\eta}-\mu}{2T}\right)\right], \tag{10}$$

and T denotes the temperature.

3. Results and Discussion

In our present analyses, all $\varepsilon_{\boldsymbol{k}\nu}$ and $z_{i\lambda}(\boldsymbol{k})$ in eq. (7) are first calculated for 64^3 $\boldsymbol{k}-$points on an equally spaced mesh in FBZ for each band. Then, we calculate $V_{ij}(\boldsymbol{k}+\boldsymbol{k}')$ in eq. (7) only for $\boldsymbol{k}-$ and $\boldsymbol{k}'-$points satisfying the conditions $\varepsilon_{\boldsymbol{k}\lambda} = \mu$ and $\varepsilon_{\boldsymbol{k}'\nu} = \mu$, respectively. When we calculate $V_{ij}(\boldsymbol{k}+\boldsymbol{k}')$ according to eqs. (9) and (10), we set the temperature $T = 0.001\,\text{eV}\sim 10\,\text{K}$, at which our system can be considered to behave similarly to that in the ground state. These calculations have been performed at $U = 0.5\,\text{eV}$, where magnetic instabilities cannot occur. We take $c_a = 0.3$ and $c_b = 0.7$ for all n. Other common parameters are summarized in Table I. In order to solve eq. (7) practically, we substitute Ψ into both sides of eq. (7) using

t_{dp}	t_{pp}	t_{dd}	$t_\perp$	Δ_{dp}
1.00 eV	−300 meV	10 meV	5 meV	2.10 eV

Table I. Transfer and hybridization gap energies.

eq. (8) and integrate for k_x, k_x', k_y, and k_y'. Thus, we reduce eq. (7) to the eigenequation for $a_\lambda(k_z)$. When we solve it numerically by the standard method, we can finally obtain both the eigenvalue, $1/\log_e\Delta_{\rm sc}$, and the eigenvector, $a_\lambda(k_z)$.

First, we summarize our results on $\Delta_{\rm sc}$ vs $\delta_{\rm h}(\delta_{\rm e})$ in Fig. 2. As discussed in our previous paper on the two-dimensional (2D) d-p model,[19] the existence of a Van Hove singularity (VHS) at the Fermi level causes a high density of states (DOS) and enhances $\Delta_{\rm sc}$. In the 2D d-p

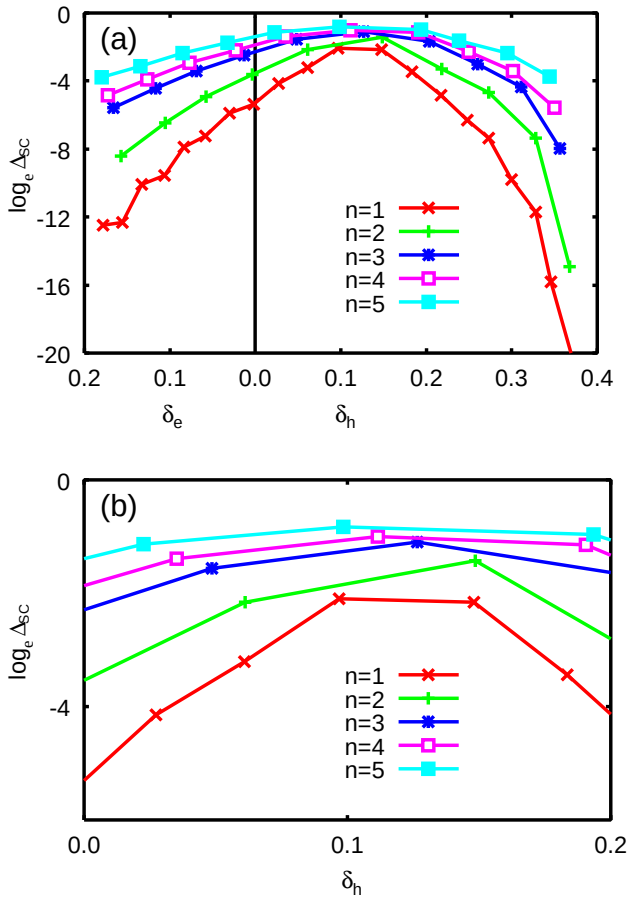

Fig. 2. (a) $\log \Delta_{sc}$ vs δ_h (hole-doped) or δ_e (electron-doped) in the cases of $n = 1, 2, 3, 4$, and 5. (b) Magnification of (a) in the region of $0.0 \leq \delta_h \leq 0.2$.

model the parts of the Fermi surface with VHS are distributed as *lines*. Therefore Δ_{sc} varies drastically in the neighborhood of the doping point at which the Fermi surface has VHS. This is in contrast with the case in the 3D d-p model. Although the energy dispersion along the c-axis introduced in our analyses is very weak, as indicated in Table I, the parts of the Fermi surface with VHS are distributed as *points*. Thus, the transition of Δ_{sc} in the 3D model is milder than that in the 2D model, as seen in Fig. 2.

Furthermore, in Fig. 2 we can clearly recognize that the enhanced Δ_{sc} prevails in a wider doping region with larger n. This result is caused by the *multilayering effect* introduced as described by eq. (4). In order to explain how the multilayering effect occurs, we show the eigensolutions, $a_\lambda(k_z)$, defined by eq.(8), and the Fermi surfaces for the cases with $n = 3, 4$, and 5 in Figs. 3, 4, and 5, respectively.

In Fig. 3 the highest amplitude of the eigensolution appears in the band with $\lambda = 2$, whose Fermi surface most closely approaches the VHS points, i.e., $(\pm\pi, 0, [-\pi, \pi])$ and $(0, \pm\pi, [-\pi, \pi])$. Thus, the band with $\lambda = 2$ has the largest DOS near VHS points and is

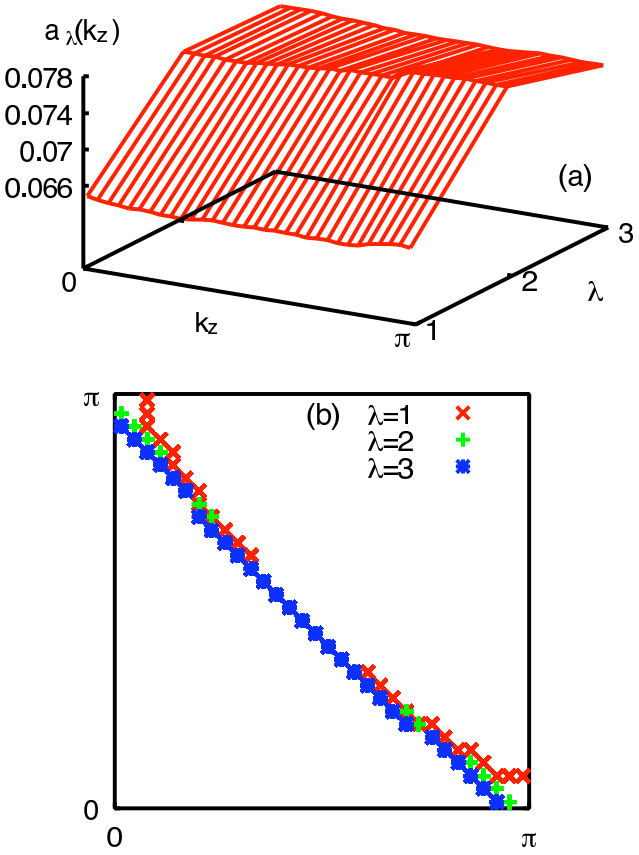

Fig. 3. The results for $n = 3$ and $\delta_{\rm h} = 0.127$. (a) The eigensolution $a_\lambda(k_z)$. (b) The Fermi surface projected onto the plane with $k_z = 0$.

dominant in the superconductivity. For the same reason, the largest amplitude of the eigensolution appears in the band with $\lambda = 3$ and in the one with $\lambda = 4$, as shown in Figs. 4 and 5, respectively.

When we change the amount of doped carriers, the Fermi surface should be transformed. As a result, another band could then have the largest DOS near the VHS points and dominate the superconductivity. This possibility should be further increased more if our model has more alternative bands. Hence, the enhanced $\Delta_{\rm sc}$ tends to prevail in a wider doping region with larger n. This tendency should remain when n becomes much larger, as long as the conventional Fermi surface can be defined. However, the largest value of $\Delta_{\rm sc}$ should be saturated toward the intrinsic value for $n \to \infty$.

Hereafter, we turn our attention to the maximum $T_{\rm c}$ of the n-layered materials, which would be proportional to the maximum $\Delta_{\rm sc}$ in our calculated results. In several real materials, the largest $T_{\rm c}$ is achieved when $n = 3$ or $n = 4$, and $T_{\rm c}$ is rather low when $n = 5$.[4,5] For such materials our assumption that the well-defined Fermi surface exists might not be valid. For example, in the five-layered compound $HgBa_2Ca_4Cu_5O_y$, the inner CuO_2 planes turn out to be antiferromagnetic on account of the strong electronic correlation.[20] Concerning the strong

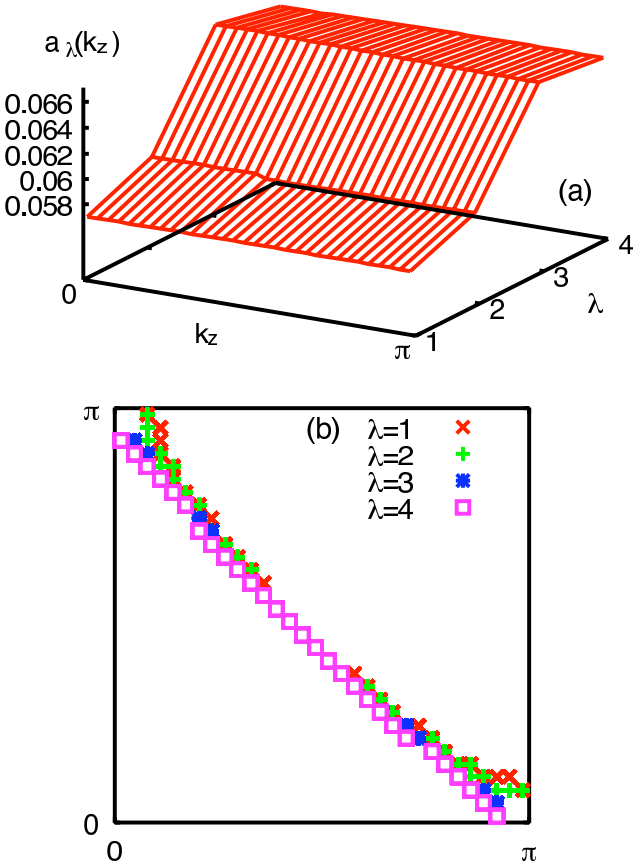

Fig. 4. The results for $n = 4$ and $\delta_{\rm h} = 0.112$. (a) The eigensolution $a_\lambda(k_z)$. (b) The Fermi surface projected onto the plane with $k_z = 0$.

electronic correlation, other theoretical works based on the 2D multilayer t-J model have been extensively carried out by Mori et al.[21,22] Their approach would be better for explaining the results for such compounds.

Although our results on $T_{\rm c}$ are not consistent with those for several real materials, our conclusion on the multilayering effect is clearly applicable to other real materials. Indeed, (Cu,C)$Ba_2Ca_3Cu_4O_{12+y}$ (Cu1234), has a high $T_{\rm c}$ even though it is in the heavily overdoped region.[1–3] Cu1234 has been revealed, by NMR experiment, to have doped holes that are almost uniformly distributed into each layer.[4,5] Thus, our assumption concerning the Fermi surface is considered to be valid for Cu1234.

4. Summary

We demonstrated that the ground state of the 3D d-p model with a multilayer perovskite structure can be in the $d_{x^2-y^2}$-wave superconducting state up to the second-order in the perturbation theory framework. In the multilayer system, the region with large $\log \Delta_{\rm sc}$ can expand further. This is caused by the multilayering effect, which can increase the chance that the Fermi surface has VHS and can maintain a high DOS around the Fermi level over a wide

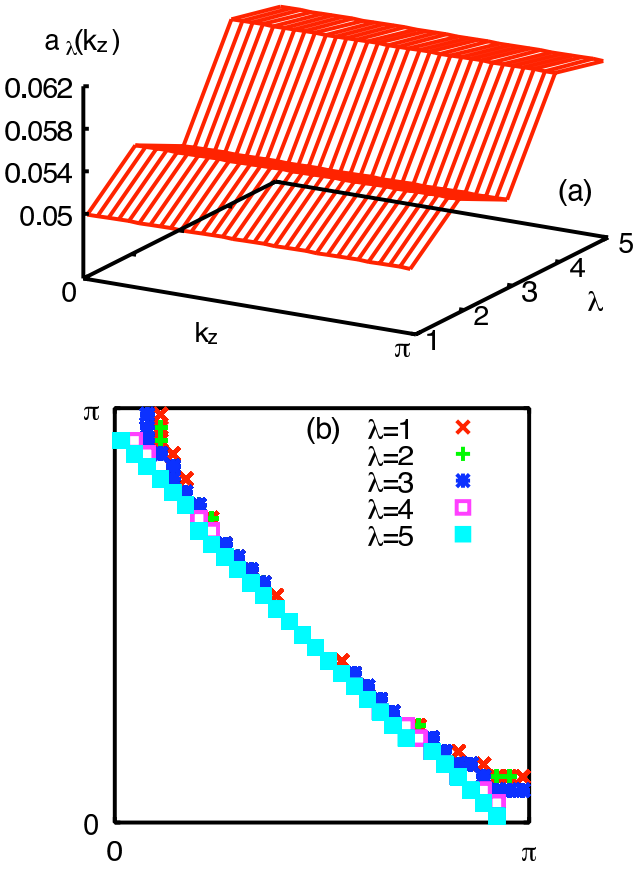

Fig. 5. The results for $n = 5$ and $\delta_{\rm h} = 0.098$. (a) The eigensolution $a_\lambda(k_z)$. (b) The Fermi surface projected onto the plane with $k_z = 0$.

doping region. This multilayering effect works very well when the unit cell contains more layers, as long as a well-defined Fermi surface exists.

Acknowledgments

The authors thank to Dr. Y. Aiura for providing his group's ARPES results and for invaluable discussions. The authors are also grateful to Professor J. Kondo and Professor K. Yamaji for their invaluable comments. S. K. also thanks Dr. M. Mori and Mr. S. Sasaki for stimulating discussions.

References

1) H. Ihara, A. Iyo, K. Ishida, N. Terada, M. Tokumoto, Y. Sekita, M. Umeda, K. Tanaka, K. Tokiwa, T. Tsukamoto and T. Watanabe: Physica C **282-287** (1997) 1973.
2) T. Watanabe, S. Miyashita, N. Ichioka, K. Tokiwa, K. Tanaka, A. Iyo, Y. Tanaka and H. Ihara: Physica B **284-288** (2000) 1075.
3) H. Ihara, A. Iyo, Y. Tanaka, N. Terada, K. Tokiwa, T. Watanabe, Y. Tokunaga, K. Ishida, Y. Kitaoka and N. Hamada: Physica B **292** (2000) 238.
4) Y. Tokunaga, K. Ishida, Y. Kitaoka, K. Asayama, K. Tokiwa, A. Iyo and H. Ihara: Phys. Rev. B **61** (2000) 9707.
5) H. Kotegawa, Y. Tokunaga, K. Ishida, G.-q. Zheng, Y. Kitaoka, H. Kito, A. Iyo, K. Tokiwa, T. Watanabe and H. Ihara: Phys. Rev. B **64** (2001) 064515.
6) Y.-D. Chuang, A. D. Gromko, A. Fedorov, Y. Aiura, K. Oka, Yoichi Ando, H. Eisaki, S. I. Uchida and D. S. Dessau: Phys. Rev. Lett. **87** (2001) 117002.
7) D. L. Feng, N. P. Armitage, D. H. Lu, A. Damascelli, J. P. Hu, P. Bogdanov, A. Lanzara, F. Ronning, K. M. Shen, H. Eisaki, C. Kim, Z.-X. Shen, J.-i. Shimoyama and K. Kishio: Phys. Rev. Lett. **86** (2001) 5550.
8) O. K. Andersen, A. I. Liechtenstein, O. Jepsen and F. Paulsen: J. Phys. Chem. Solids **56** (1995) 1573.
9) N. Bulut, D. J. Scalapino and R. T. Scalettar: Phys. Rev. B **45** (1992) 5577.
10) R. T. Scalettar, J. W. Cannon, D. J. Scalapino and R. L. Sugar: Phys. Rev. B **50** (1994) 13419.
11) A. I. Liechtenstein, O. Gunnarsson, O. K. Andersen and R. M. Martin: Phys. Rev. B **54** (1996) 12505.
12) W. Kohn and J. M. Luttinger: Phys. Rev. Lett. **15** (1965) 524.
13) D. Fay and A. Layzer: Phys. Rev. Lett. **20** (1968) 187.
14) S. Nakajima: Prog. Theor. Phys. **50** (1973) 1101.
15) P. W. Anderson and W. F. Brinkman: Phys. Rev. Lett. **30** (1973) 1108.
16) M. Yu. Kagan and A. V. Chubukov: JETP Lett. **47** (1988) 614.
17) R. Hlubina: Phys. Rev. B **59** (1999) 9600.
18) J. Kondo: J. Phys. Soc. Jpn. **70** (2001) 808.
19) S. Koikegami and T. Yanagisawa: J. Phys. Soc. Jpn. **70** (2001) 3499; **71** (2002) 671(E).
20) H. Kotegawa, Y. Tokunaga, Y. Araki, G.-q. Zheng, Y. Kitaoka, K. Tokiwa, K. Ito, T. Watanabe, A. Iyo, Y. Tanaka and H. Ihara: Phys. Rev. B **69** (2004) 014501.
21) M. Mori, T. Tohyama and S. Maekawa: Phys. Rev. B **66** (2002) 064502.
22) M. Mori, T. Tohyama and S. Maekawa: Physica C **388** (2003) 51; **392-396** (2003) 123; **378** (2002) 333.